ACS OMEGA

Open Access

http://pubs.acs.org/journal/acsodf

Article

Influence of the 3-Hydroxyvalerate Content on the Processability, Nucleating and Blending Ability of Poly(3-Hydroxybutyrate-*co*-3-hydroxyvalerate)-Based Materials

Sara Alfano, Estelle Doineau, Coline Perdrier, Laurence Preziosi-Belloy, Nathalie Gontard, Andrea Martinelli, Estelle Grousseau, and Hélène Angellier-Coussy*

Cite This: *ACS Omega* 2024, 9, 29360−29371

Read Online

ACCESS | Metrics & More | Article Recommendations | Supporting Information

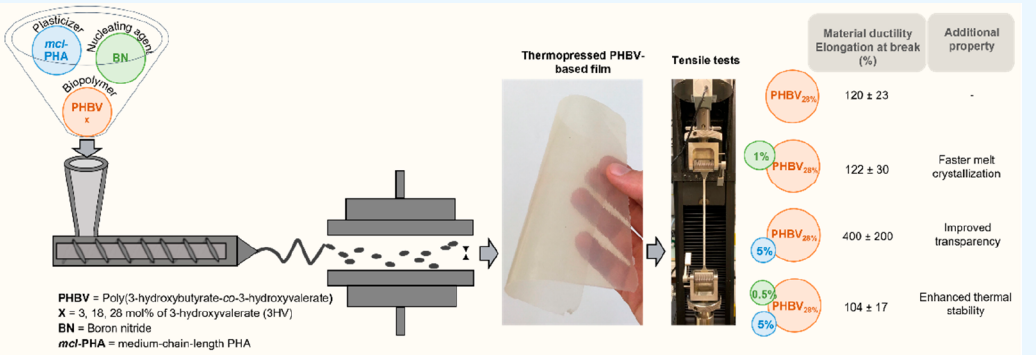

ABSTRACT: Poly(3-hydroxybutyrate-*co*-3-hydroxyvalerate (P(3HB-*co*-3HV) copolymers are an attractive class of biopolymers whose properties can be tailored by changing the 3-hydroxyvalerate monomer (3HV) concentration, offering the possibility of counteracting problems related to high crystallinity, brittleness, and processability. However, there are few studies about the effects of 3HV content on the processability of copolymers. The present study aims to provide new insights into the effect of 3HV content on the processing step including common practices like compounding, addition of nucleation agents and/or amorphous polymers as plasticizers. P(3HB-*co*-3HV)-based films containing 3, 18, and 28 mol % 3HV were processed into films by extrusion and subsequent molding. The characterization results confirmed that increasing the 3HV content from 3 to 28 mol % resulted in a decrease in the melting point (from 175 to 100 °C) and an improvement in mechanical properties (i.e., elongation at break from 7 ± 1% to 120 ± 3%). The behavior of P(3HB-*co*-3HV) in the presence of additives was also investigated. It was shown that an increase in the 3HV content leads to better miscibility with amorphous polymers.

INTRODUCTION

Polyhydroxyalkanoates (PHAs) are a class of biodegradable polyesters[1] produced by microorganisms in both pure and mixed cultures, fed with synthetic volatile fatty acid mixtures or from low-cost feedstocks, including organic fraction of municipal solid waste (OFMSW),[2] waste-activated sludge (WAS)[3] or other byproducts of the agrifood industry.[4,5] They are categorized into two main groups: (1) *short chain length*-PHA (*scl-PHA*), having 0−2 carbon atoms in the side chain and (2) *medium chain length*-PHA (*mcl-PHA*), with 3−11 carbon atoms in the side chain and characterized by mechanical properties similar to that of rubber and elastomer.[6,7] Poly(3-hydroxybutyrate) (P3HB) and its copolymer poly(3-hydroxybutyrate-*co*-3-hydroxyvalerate) (P(3HB-*co*-3HV)) are the most widespread PHAs, belonging to the first group. Thermal and mechanical behavior depends on the 3-hydroxyvalerate (3HV) monomeric concentration. In general, copolymers with low 3HV content (0−17 wt %% 3HV) are brittle and stiff due to their high crystallinity (value of respectively 80 and 63% for P3HB and P(3HB-*co*-3HV with 17 wt % 3HV[8])). They also have a melting point (ranging from 160 to 180 °C)[8] close to the beginning of the thermal degradation (occurring between 170 and 200 °C[9]), which makes their processability very tricky. In addition, the slow crystallization rate and low nucleation density favor the formation of large spherulites leading to easier cracks and fracture, as indicated by the low elongation at break values of 2−7%.[10,11] P3HB and P(3HB-*co*-3HV) undergo secondary

Received: February 9, 2024
Revised: April 14, 2024
Accepted: April 23, 2024
Published: June 27, 2024

crystallization phenomena which lead to progressive embrittlement and changes in properties over time.[12]

One approach to counter these drawbacks is to prepare P(3HB-*co*-3HV) with different contents of 3HV units, by adjusting production process parameters such as microbial culture feeding strategies.[13,14] An increase in 3HV percentage molar content (mol %) from 0 to 100 mol % resulted in a larger amorphous region and then a linear decrease of the glass transition temperature. The melting temperature and crystallinity are lowered by increasing the 3HV content up to 45 mol %.[15] This compositional range corresponds to the pseudoeutectic point at which crystallinity and melting temperature reach the minimum value.[16−18]

Copolymers with an increased 3HV content are thus characterized by higher flexibility and toughness. For example, elongation at break values of 62% and 26% were measured for P(3HB-*co*-3HV) with a 3HV content of 18 mol %.[19] Worth noting that such results were obtained on films prepared using a simple thermopressing step of the polymer powders. No information about the effect of a preliminary compounding step by melt extrusion, commonly used in the plastics industry, has been reported yet for copolymers with greater 3HV content, but it is reasonable to assume that processing has a strong impact on the structure of materials, which itself influences the resulting mechanical properties.

However, it has been observed that P(3HB-*co*-3HV) copolymers with a high 3HV (over 40 mol %) content show very slow crystallization rates[19,20] making them unsuitable for industrial applications if used as main constituent. The low crystallization rate results in time-consuming solidification steps after extrusion, making the entire process less efficient than that for fossil-based plastics. The addition of a nucleating agent to polymers is a common method to ensure rapid crystallization, controllable, and homogeneous spherulite size and to limit secondary crystallization. At that time, many efforts were made to improve the performance of P(3HB-*co*-3HV) by studying the effect of various fillers and nucleating agents, including boron nitride (BN), organoclays and cellulose nanocrystals (CNCs), on the crystallization and mechanical behavior of the compounded materials.[21−24] However, such studies have been performed exclusively with commercially available P(3HB-*co*-3HV) with low 3HV content (e.g., 3HV content of about 0−8 mol %). No information about the impact of nucleation agent addition on P(3HB-*co*-3HV) with higher 3HV content are available.

To further enhance the P(3HB-*co*-3HV) properties they were blended with synthetic and natural polymers, including polysaccharides such as starch[25] natural rubber,[26,27] and other polyesters such as poly(lactic acid) (PLA).[28,29] P(3HB-*co*-3HV) copolymers have also been blended with other PHAs like poly(3-hydroxybutyrate-*co*-3-hydroxyhexanoate) (PHBHHx)[30,31] or amorphous *mcl*-PHA.[31] To obtain significant improvements in the physical−chemical and mechanical properties, great attention must be paid to the formulation and processing conditions to avoid phase segregation phenomena, which could lead to a decrease in the general performance of the material. Quite all studies about blending demonstrate the necessity of using a compatibilizer or a cross-linker like grafting with glycidyl methacrylate[32] or dicumyl peroxide[33] to allow the miscibility of P3HB or P(3HB-*co*-3HV) (<8 mol % 3HV) with other polymers. One of the possible causes of poor miscibility is the high inherent crystallinity of the 3HV-poor P(3HB-*co*-3HV), which leads to the formation of crystalline domains and segregation phenomena. The presence of more 3HV units, thanks to the increase in the amorphous fraction, may favor blending with other polymers. However, no study has yet been carried out on the blending of P(3HB-*co*-3HV) copolymers with an increased 3HV content; therefore, there is a lack of knowledge.

In this context, the present paper aims to fill the knowledge gap on copolymers with different 3HV content by answering the following three questions:

- How can the melt extrusion process affect the final mechanical properties of P(3HB-*co*-3HV)-based materials with increased 3HV content?
- How does the increased 3HV content affect the nucleating effect of BN (which is already well-known for P3HB and P(3HB-*co*-3HV) with a low 3HV content)?
- How does the increased 3HV content affect the ability of P(3HB-*co*-3HV) to be blended with toughening additives such as *mcl*-PHAs?

For this purpose, three P(3HB-*co*-3HV) copolymers were compounded with different amounts of BN (0.5, 1, and 2 wt %), used as nucleating agent, and/or *mcl*-PHA (5 wt %), used as toughening additive. The 3HV contents of the investigated copolymers were 3, 18, and 28 mol %. The monomeric composition has been chosen to evaluate the behavior of low (3 mol %) and moderate (18 and 28 mol %) 3HV contents. Copolymers with a higher 3HV content (i.e., 40 mol %) were not investigated because their low crystallization rate limits the possibility of rapid processing. The virgin polymer and mixtures were extruded, pelletized, and compressed in 100 μm thick films. The effect of the processing conditions and the formulation on the thermal and the mechanical properties of P(3HB-*co*-3HV)-based films was investigated by differential scanning calorimetry (DSC), thermogravimetric analysis (TGA) and tensile tests. Finally, water vapor permeability (WVP) measurements were performed to verify whether the monomeric composition and the presence of additives affected the barrier properties of P(3HB-*co*-3HV)-based films for packaging applications.

MATERIALS AND METHODS

Materials. P(3HB-*co*-3HV) containing approximately 1−3 mol % of 3-hydroxyvalerate units (3HV) was purchased from NaturePlast under the reference PHI003 in the form of a very fine powder without any additive. It is noted that PHBV3 is in the present study. P(3HB-*co*-3HV) copolymers with 18 and 28 mol % of 3HV units (denoted PHBV18 and PHBV28, respectively) were produced by UMR IATE (Montpellier, France) in the framework of the ANR LOOP4PACK project, as reported in ref 34 and extracted using a solvent-free high pressure homogenization (HPH) based method.[19] It was shown in a previous study[19] that the three copolymers considered in the study crystallized in the P(3HB) crystalline lattice. Wide-angle X-ray analysis showed that the three lattice parameters undergo a moderate but gradual increase by increasing the 3HV molar fraction, showing an expansion of crystals in all directions that was ascribed to the inclusion of 3HV units within the P(3HB) crystals.

Boron nitride (BN) in the form of fine powder (purity of 98%, particle size of 1 μm) purchased from Sigma-Aldrich was used as a nucleating agent. The *mcl*-PHA, containing 70 wt % of 3-hydroxynonanoate (3HN), 29 wt % of 3-hydroxyepta-

https://doi.org/10.1021/acsomega.4c01282
ACS Omega 2024, 9, 29360−29371

noate (3HHp) and 1 wt % of 3-hydroxyvalerate (3HV) units, was purchased from Versamer (Canada) in the form of a single sticky block under the reference PHN970. Repeating units of used PHAs are reported in Figure 1.

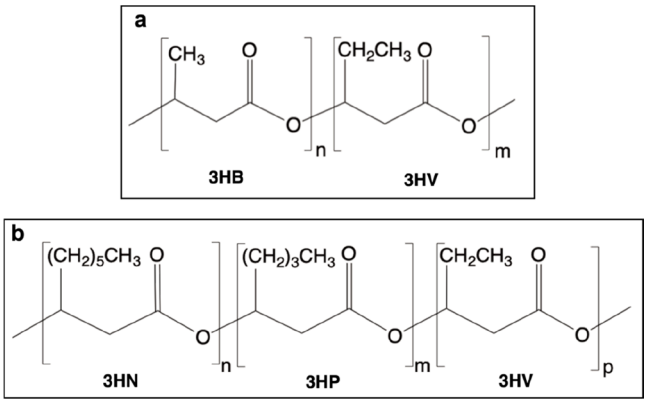

Figure 1. Chemical structure of (a) P(3HB-*co*-3HV) and (b) mcl-PHA copolymers.

Before compounding, *mcl*-PHA was reduced in powder form by crushing the block in liquid nitrogen. The resulting powder was further dried at 25 °C in a vacuum oven for 24 h.

Intrinsic physical-chemical characteristics of all used polymers are summarized in Table 1.

Methods. *Preparation of P(3HB-co-3HV)-Based Films.* P(3HB-*co*-3HV) powders were mixed with 5 wt % of *mcl*-PHA and either 0.5, 1, and 2 wt % of BN, by manual agitation for 2 min. The codification of samples is given in Table 2. Before compounding, the mixtures were dried at 25 °C under a vacuum for 24 h to eliminate traces of humidity and limit thermodegradation phenomena during processing. In the case of virgin P(3HB-*co*-3HV), samples were dried at 50 °C under a vacuum for 24 h. The compounding step was carried out by melt extrusion using a Process 11 thin screw extruder (Thermo Scientific, Germany) with a L/D of 40, a screw diameter of 11 mm, and a 3 mm rod die. The temperature profile has been adjusted according to the melting point of P(3HB-*co*-3HV)s, i.e., 130−160−180−180−180 °C for PHBV3 and 130−130−160−160−160 °C for PHBV18 and PHBV28 from the feeder to the die. The polymer was fed manually, and the screw speed was 150 rpm. The extruded rods were cooled to room temperature and pelletized using a granulator (Thermo Scientific, Germany). Resulting compounds were dried at 25 °C under a vacuum for 24 h before being pressed in films using a heating hydraulic press (20T, Pinette Emidecau Industries, Chalon-sur-Saône, France). For that purpose, 2.2 g of pellets were heated between two Teflon coated films in a 100 μm thick mold to obtain films of 12 × 12 cm^2 following 4 processing steps: contact with plates at heating temperature for 5 min, then pressing from 50 to 100 bar at heating temperature during a period time of 1 min, then applying a pressure of 150 bar for 1 min and finally cooling during 10 min under a constant weight of 1 kg. Different heating temperatures were used for the preparation of the films, depending on the sample formulation. PHBV3 was pressed at 180 °C while PHBV18 and PHBV28 were pressed at both 160 and 170 °C, to evaluate the impact of the heating temperature on final material properties.

In the case of virgin polymers, films were also produced directly from powders by skipping the compounding step. Nonextruded samples were noted as PHBV3_ne, PHBV18_ne and PHBV28_ne.

All of the films were stabilized at 25 °C and 50% HR for 14 days prior to further characterization to allow cold crystallization to occur and maximum crystallinity to be achieved.

Thermal Characterization. Thermal properties of produced materials have been investigated through differential Scanning Calorimetry (DSC) analyses using a TA Instruments (Q200 modulated DSC, TA Instruments, New Castle, USA) calorimeter under a nitrogen atmosphere with a flow rate of 50 mL min^{-1}. The temperature program was the following: a first heating scan from −30 to 190 °C, cooling scan until −30 °C, and a second heating scan from −30 to 190 °C. All the scans were conducted at a heating rate of 10 °C min^{-1}. Around 12 mg of sample was used for each analysis. Melting enthalpies were used as an indicator of crystallinity because of the lack of ΔH_m^0 for P(3HB-*co*-3HV) copolymers with higher 3HV content making it impossible to calculate the crystallinity degree (%) as the ratio between ΔH_m of sample and ΔH_m^0. The shifting in melt crystallization temperature (noted T_{mc}) has been calculated according to eq 1 and has been taken as an indication of the BN nucleation efficiency in P(3HB-*co*-3HV) nucleated samples. Measurements were done at least in triplicate.

$$\Delta T_{mc} = T_{mc}(\text{nucleated PHBV}) - T_{mc}(\text{neat PHBV}) \quad (1)$$

Thermal stability has been studied by TGA using a Mettler TGA2 device (Schwerzebbach, Switzerland) equipped with an XP5U balance. Samples were heated from 25 to 600 °C at 10 °C min^{-1} under nitrogen flow of 50 mL min^{-1} and results were analyzed using STARe software.

The onset temperatures (T_d^{onset}) and the maximum degradation temperature (T_d), corresponding to the temperature at which the first derivative of the weight loss became

Table 1. Physical−Chemical Characteristics of the Materials Used in This Study: Purity, Molecular Weight (MW), Melting Temperature (T_m), Glass Transition Temperature (T_g) and Crystallinity Degree[a]

sample	purity (%)	MW (kg mol^{-1})	T_m (°C)	T_g (°C)	crystallinity degree (%)
PHBV3	n.p.	1124	174.3 ± 0.2[c]	1.2 ± 0.1[c]	69 ± 3[c]
PHBV18	95	935 ± 25[b]	120.8 ± 0.0[b]	1.0 ± 0.2[b]	63 ± 1[b]
			174.4 ± 0.0[b]	64.5 ± 0.1[b]	
PHBV28	98	1075 ± 14[b]	94.5 ± 0.5[b]	−4.4 ± 1.4[b]	55 ± 1[b]
			173.5 ± 1.2[b]	52.8 ± 0.4[b]	
mcl-PHA	n.p.	104	46	−40	n.d.

[a]Multiple T_m values for the same sample are reported on different lines, as in the case of T_g. n.p. = not provided. [b]From Doineau et al.[19] [c]From Bossu et al.[35]

https://doi.org/10.1021/acsomega.4c01282
ACS Omega 2024, 9, 29360−29371

Table 2. Codification of the Samples

neat polymer	+0.5 wt % BN	+1 wt % BN	+2 wt % BN	+5 wt % *mcl*-PHA	+0.5 wt % BN + 5 wt % *mcl*-PHA
PHBV3	PHBV3_0.5BN	PHBV3_1BN	PHBV3_2BN	PHBV3_5mcl	PHBV3_0.5BN_5mcl
PHBV18	PHBV18_0.5BN	PHBV18_1BN	PHBV18_2BN	PHBV18_5mcl	PHBV18_0.5BN_5mcl
PHBV28	PHBV28_0.5BN	PHBV28_1BN	PHBV28_2BN	PHBV28_5mcl	PHBV28_0.5BN_5mcl

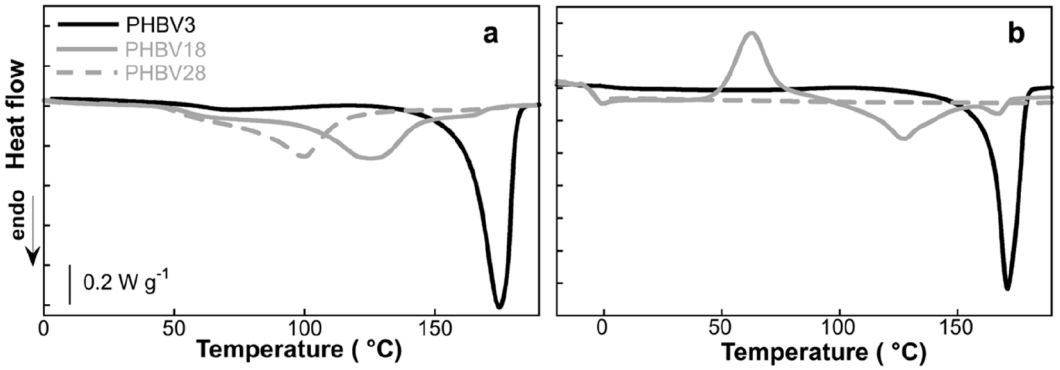

Figure 2. First (a) and second (b) heating scans of the PHBV3, PHBV18, and PHBV28 pellets.

higher than 0.1% $°C^{-1}$ and lower than 0.1% $°C^{-1}$ and to the one at which the degradation rate is maximum, respectively, have been taken in consideration. Simulated TGA traces of the PHBV/*mcl*-PHA blend have been plotted by applying the additive rule and used for compatibility evaluation. The eq 2 used is the following:

$$W_{A-B} = (1 - x)W_A + xW_B \quad (2)$$

where W is the TGA curve, A and B are the components of the blend, and x is the weight fraction of component B.

Tensile Tests. The tensile tests were carried out on dumbbell shaped specimens. The dimensions of the specimens were 4 mm in width, and 22 mm in effective length (L_0). The distance between the jaws was 45 mm. The tests were performed using an Instron 68SC-5 machine equipped with a 50 N cell and at a crosshead speed of 10 mm min^{-1}. Ten repetitions were characterized for each formulation.

Polarized Optical Microscope Measurements (POM). Polarized optical microscopy (POM) analysis was made by using an Optiphot2-Pol light microscope (Nikon) equipped with a Linkam HFS 91 hot stage (Linkam, Tadworth, UK) driven by a Linkam TP 92 temperature controller. The images were acquired with a Nikon D7200 camera. Little pieces of both nucleated and neat P(3HB-*co*-3HV) films were melted between two glass slides and cooled to room temperature directly on the hot stage. Pictures were acquired after 2 weeks of stabilization at 25 °C.

Scanning Electron Microscopy (SEM). The morphology of liquid nitrogen fractured PHBV_5mcl and virgin PHBV pellets was investigated by scanning electron microscopy using a field emission scanning electron microscope (AURIGA, Zeiss, Jena, Germany). Prior to the measurements, the samples were sputtered with gold.

Water Vapor Permeability. Water vapor permeability (WVP) was determined at 23 °C by using a gravimetric method. Films (five repetitions) were hermetically sealed with a Teflon seal in glass permeation cells containing distilled water. These cells were placed in a desiccator containing silica gel (RH of around 3%). They were weighed using a four-digit balance (BALCO − Type LX 220A, Switzerland) at regular intervals for 7 days. It was checked that the PHBV films did not swell during the experiment. Water vapor permeability was calculated from the following eq 3:

$$WVP = \frac{S \times t}{A \times \Delta P} \quad (3)$$

where S is the slope of the weight change from the straight line ($mol \cdot s^{-1}$), A is the permeation area (m^2), t is the average specimen thickness (m), and ΔP is the water vapor pressure differential across the film (Pa).

RESULTS AND DISCUSSION

Effect of 3HV Content on Processability and Mechanical Properties. It is largely described in literature that increasing 3HV content results in higher ductility due to the formation of smaller and homogeneous spherulites[6,36] Recently, an in-depth DSC analysis of HPH-recovered P(3HB-*co*-3HV)s combined with mechanical testing allowed identifying an optimal processing temperature for each grade of P(3HB-*co*-3HV).[19] These results were collected on films prepared by simple thermopressing of the polymer powders, i.e., without considering possible shearing effects that may occur during an upstream compounding step by melt extrusion. In this context, this work aimed to evaluate the effects of an additional compounding step impact on the final mechanical properties of P(3HB-*co*-3HV)-based materials with increased 3HV content.

Regardless of the monomeric composition, it was possible to obtain continuous rods of P(3HB-*co*-3HV) thanks to their high molecular weight (Table 1). However, the ability to pelletize the rods depended on the 3HV content. In fact, unlike PHBV3, which crystallizes rapidly, PHBV18 and PHBV28 were sticky upon exiting the die and required stabilization for at least 30 min before the granulation. This behavior is the consequence of the different crystallization rates of copolymers, which are very low for PHBV18 and PHBV28 samples as evidenced by Doineau et al.[19] The thermograms relative to the first and second heating scans of pellets are displayed in Figure 1 and the temperature and enthalpy of the observed transitions are reported in Table S1, Supporting Information. The first scan confirmed that the melting temperature T_m decreased with increasing 3HV content, from 174 °C for PHBV3 to 94 °C for

https://doi.org/10.1021/acsomega.4c01282
ACS Omega 2024, 9, 29360−29371

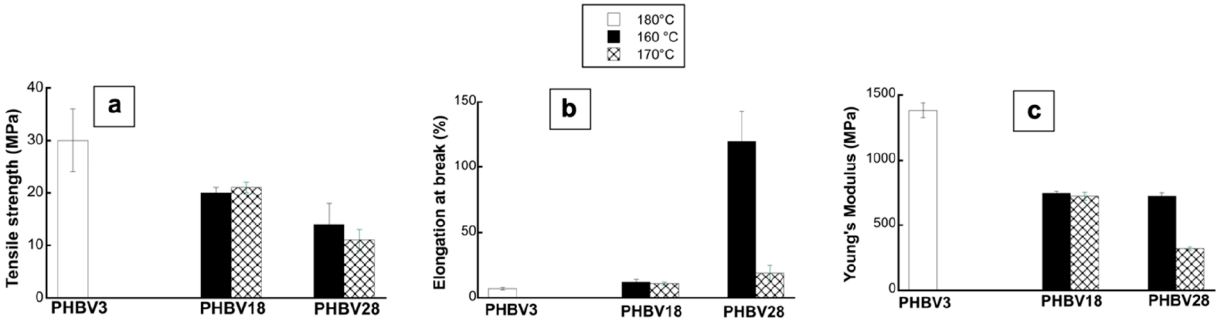

Figure 3. (a) Tensile strength (MPa), (b) elongation at break (%), and (c) Young's Modulus (MPa) of PHBV3, PHBV18, and PHBV28 films prepared from compounded pellets and thermopressed at 160, 170, and/or 180 °C.

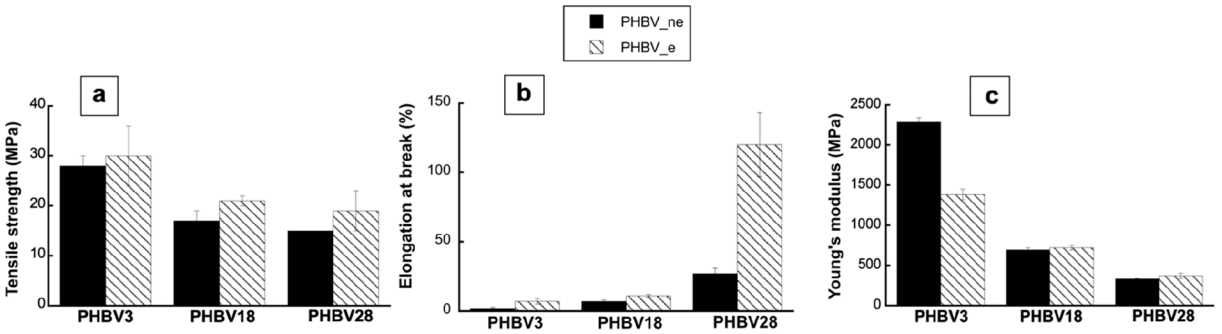

Figure 4. (a) Tensile strength (MPa), (b) elongation at break (%), and (c) Young's modulus (MPa) of P(3HB-*co*-3HV) films obtained by thermopressing at 160 °C either powders (PHBV_ne) or compounded pellets (PHBV_e).

PHBV28 (Table 1, Figure 2a). When polymers were heated to 190 °C, melt crystallization was hindered for P(3HB-*co*-3HV) with increased 3HV content (Figure S1, Supporting Information) due to the difficulty for P(3HB-*co*-3HV) to reach a new ordered system when all the nuclei are eliminated, especially because of a drop of viscosity that hinders heterogeneous nucleation.[19] PHBV18 pellets melt crystallize partially at T_{mc} = 39 °C with a very low enthalpy (ΔH_{mc} = 1.3 ± 0.4 J g^{-1}) and underwent a further substantial cold-crystallization (ΔH_{cc} = 36 J g^{-1}) only in the following heating at a temperature of about T_{cc} = 62 °C (Figure 2b). PHBV28 showed no melting nor cold crystallization, remaining amorphous at the end of the cooling, as revealed by the absence of a melting peak during the second heating (Figure 2b). The crystallization process of PHBV18, occurring in two stages (melt and cold crystallization), implies the formation of spherulites under different conditions, characterized by different morphologies and dimensions. Differently, PHBV3 completely crystallized upon cooling, not showing further crystallization in the subsequent heating scan.

The thermal stability of pure copolymers was evaluated by TGA experiments, which showed that the main thermal degradation temperature of the P(3HB-*co*-3HV) pellets decreased from 264 °C for PHBV3 down to 223 and 234 °C for PHBV18 and PHBV28, respectively (Table S1, Supporting Information). It is worth noting that the increase in the thermal degradation temperature along with the decrease in melting temperatures for PHBV28 helps to extend the processing window.

Since it is known that the processing temperature and thermal history generally affect the crystallization mechanisms, and consequently the resulting microcrystalline structure and mechanical properties, PHBV18 and PHBV28 films were prepared at the optimum processing temperatures (160 and 170 °C) determined in a previous work.[19] In this way, the effect of thermopressing temperatures on the mechanical properties of P(3HB-*co*-3HV) films submitted to a double thermal treatment (first melt extrusion to produce compounds, then thermopressing step to produce films) was determined (Figure 3).

Due to their high crystallinity, films made of PHBV3 exhibited a low elongation at break (7 ± 1%), together with high tensile strength (30 ± 6 MPa) and Young's Modulus values (1383 ± 55 MPa). Increasing the 3HV content from 3 to 18% resulted in a general decrease of tensile strength (20 ± 1 and 21 ± 1 MPa for PHBV18 thermopressed respectively at 160 and 170 °C), a slight improvement of the elongation at break (12 ± 2% and 11 ± 1% for PHBV18 thermopressed respectively at 160 and 170 °C) and a decrease of the Young's modulus (746 ± 15 and 721 ± 31 MPa for PHBV18 thermopressed at 160 and 170 °C). For PHBV28 thermopressed at 160 °C, a huge increase of the elongation at break up to 120 ± 23% was noticed.

The thermopressing temperature, i.e., 160 or 170 °C, had no significant effect on the mechanical properties of PHBV18 films, while all mechanical properties of PHBV28 films were worsened as the thermopressing temperature increased by only 10 °C. The thermal degradation could be associated with the formation of oligomers, which make PHBV28 films more brittle. This observation led to the conclusion that the beneficial effect of increasing the 3HV content may be negatively counterbalanced by an inappropriate choice of the processing temperature.

Data collected for films thermopressed at 160 °C were compared with those produced at the same temperature but by a simple thermopressing of powders (without a preliminary compounding step) to evaluate the effect of additional thermal treatment and shearing stresses caused by the melt extrusion

https://doi.org/10.1021/acsomega.4c01282
ACS Omega 2024, 9, 29360−29371

step (Figure 4). Interestingly, both the tensile strength and elongation at break of films obtained by thermopressing compounded pellets were globally higher than that of films directly obtained from powders (Figure 4a and 4b). The increase in elongation at break was very low for PHBV3 (from 2 ± 1% to 7 ± 2%) and PHBV18 (from 7 ± 1 to 12 ± 1%), while it was huge for PHBV28 (from 27 ± 4 to 120 ± 23%). The Young's modulus was decreased for PHBV3 (from 2285 ± 57 to 1383 ± 67 MPa), while it was slightly increased for PHBV18 (from 695 ± 224 to 721 ± 29 MPa) and PHBV28 (from 334 ± 6 to 371 ± 31 MPa). The improvement in ductility observed for extruded samples was ascribed to favored chain entanglement induced by shear forces occurring during extrusion.

Although increasing the 3HV content has the advantage of reducing the brittleness and increasing the processing window, it has the side effect of reducing the crystallization rate and, hence, the rapid solidification of the material in the processing stages. The low crystallization rate also means that the materials crystallize for a long time after melt processing, possibly through different and uncontrollable stages. This could favor the formation of different crystal structures and morphologies that render the properties of P(3HB-*co*-3HV) unpredictable and unstable. The next section therefore addresses the addition of boron nitride as a nucleating agent, which has been widely used for P3HB and P(3HB-*co*-3HV) with low 3HV content and aims to evaluate how the increased 3HV content impacts the nucleating effect of BN.

Effect of BN Addition. One of the major challenges in processing P(3HB-*co*-3HV) is to prepare compounds with improved processability by accelerating melt crystallization. For that purpose, PHBV3, PHBV18, and PHBV28 were mixed with different concentrations of BN, which was used as a nucleating agent. The thermal properties (Table 3) were evaluated by DSC and TGA measurements (DSC and TGA curves are reported in Figure S2−S7 Supporting Information).

Table 3. Melting Enthalpies from First Heating Scan (ΔH_m), Nucleation Efficiency (ΔT_{mc}), and Onset Thermal Degradation Temperatures (T_d^{onset}) of Virgin and Nucleated P(3HV-*co*-3HV)s

sample	ΔH_m (J·g^{-1})	ΔH_{mc} (J·g^{-1})	ΔT_{mc} (°C)	T_d^{onset} (°C)
PHBV3	87.2 ± 0.8	75.8 ± 0.9	–	264 ± 1
PHBV18	29.6 ± 0.8	1.3 ± 0.5	–	223 ± 1
PHBV28	21.1 ± 1.6	0.4 ± 0.2	–	234 ± 3
PHBV3_0.5BN	96.7 ± 0.7	87.0 ± 1.2	24	280 ± 1
PHBV18_0.5BN	28.7 ± 0.1	41.7 ± 1.0	30	242 ± 10
PHBV28_0.5BN	20.5 ± 0.5	0.4 ± 0.2	0	263 ± 2
PHBV18_1BN	27.1 ± 0.5	41.5 ± 1.1	33	225 ± 6
PHBV28_1BN	15.7 ± 2.5	1.6 ± 0.5	9	263 ± 1
PHBV28_2BN	19.1 ± 1.0	0.6 ± 0.1	6	259 ± 7

The nucleation efficiency (NE) is usually evaluated based on the self-nucleating theory.[37,38] In this work, NE of different BN amounts has been estimated by considering only the shifting of melt crystallization temperature toward higher temperature (named ΔT_{mc}) as an indicator of nucleation ability.

As already reported for P(3HB-*co*-3HV) with low 3HV content,[39,40] the addition of only 0.5 wt % of BN in PHBV3 resulted in an increase of the melt crystallization for PHBV3 and PHBV18 while it has no significant effect on PHBV28 (Table 3). For PHBV3 and PHBV18, such a BN content was sufficient to avoid two-stage crystallization since no cold crystallization was observed (Figure S2c, Supporting Information). POM observations confirmed the efficiency of the addition of a low amount of BN to reach smaller spherulites in the case of PHBV3, passing from 140 μm for neat PHBV3 to about 10 μm for PHBV3_0.5BN. Conversely, the morphology and dimensions of PHBV18 and PHBV28 spherulites were not affected. The lower dimension of neat PHBV18 and PHBV28 spherulites (Figures 5c and 5e), around the order of magnitude

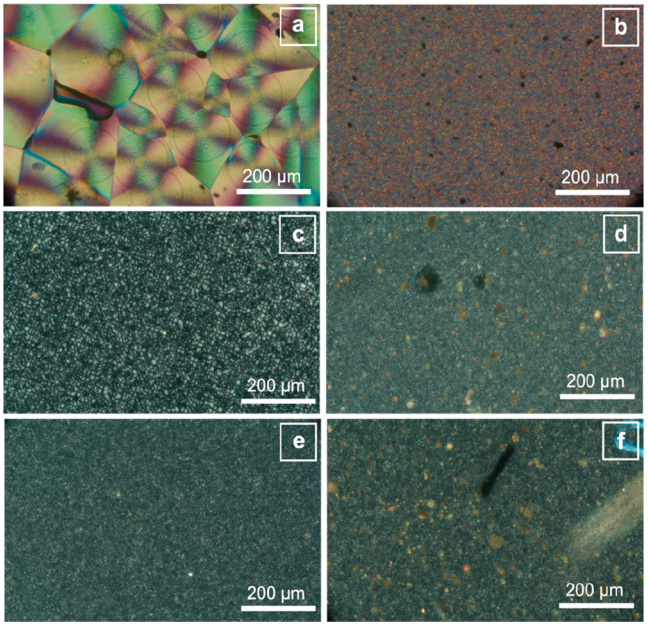

Figure 5. POM images (mag 20×) of virgin and nucleated P(3HB-*co*-3HV)s with 0.5 wt % of BN. (a) PHBV3, (b) PHBV3_0.5, (c) PHBV18, (d) PHBH18_0.5, (e) PHBV28, (f) PHBV28_0.5.

of 13 and 9.5 μm respectively, makes it difficult to notice changes in dimension and structures. It is worth noting that the lower dimensions of virgin PHBV18 and PHBV28 spherulites could be ascribed to the presence of impurities derived from the extraction process, which could act as nucleating agents.[19]

Since 0.5 wt % BN was not sufficient to ensure shorter crystallization times for P(3HB-*co*-3HV) enriched in 3HV units, additional formulations with increasing BN amounts were prepared. The ΔT_{mc} values demonstrated a greater ability of 1 wt % BN to allow faster crystallization in PHBV28 (ΔT_{mc} = 9 °C), while PHBV18 showed quite a constant value (Table 3). PHBV28 was mixed with even more BN (2 wt %), but no noticeable change was detected. The obtainment of constant ΔT_{mc} values for PHBV18_1BN and PHBV28_2BN may be caused by the aggregation of the BN particles. Although the addition of a higher BN content (1 wt %) improved crystallization when the 3HV content increased, PHBV28 still showed slow crystallization from the melt.

PHBV3 and PHBV18 thermal stability was not affected by the presence of BN since there was no significant shift in thermal degradation temperatures, according to the results shown in Miao et al.'s work.[21] In contrast, PHBV28 T_d^{onset} values increased according to added BN amount, reaching a quite constant value at higher % wt BN because of filler aggregation as in the case of PHBV/clay nanocomposites in Chen et al.'s work,[41] confirming DSC results. Improvement in

https://doi.org/10.1021/acsomega.4c01282
ACS Omega 2024, 9, 29360−29371

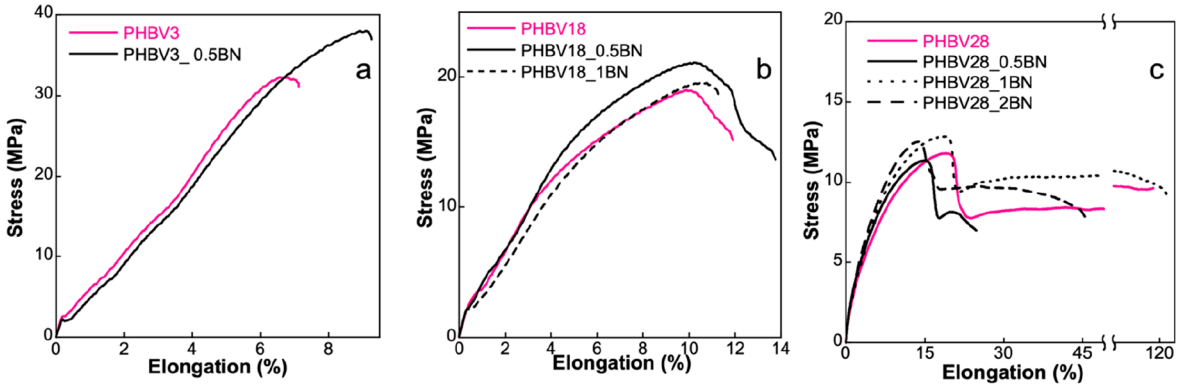

Figure 6. Stress−elongation curves of virgin and nucleated PHBV3 (a), PHBV18 (b), and PHBV28 (c) films.

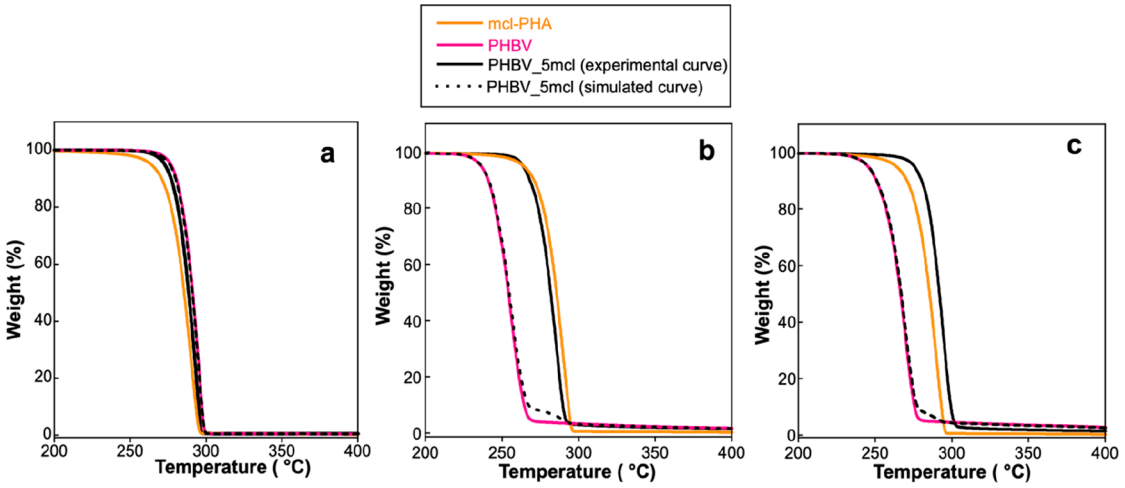

Figure 7. Comparison between experimental and simulated TGA curves of PHBV_mcl blends and pure components: (a) PHBV3, (b) PHBV18, and (c) PHBV28.

thermal stability may be attributed to BN's strong thermal conductivity and capacity to prevent local heat accumulation, which delays the generation of degradation byproducts and protects the polymeric matrix from thermodegradation. Additionally, according to Yu et al.'s research, the inclusion of BN may limit the thermal motion of polymer chains and enhance thermal stability.[42]

The impact of BN addition on mechanical properties was assessed through uniaxial tensile tests; the obtained stress−strain curves are shown in Figure 6.

Although the PHBV3 crystallinity degree did not change when 0.5 wt % BN was added, a slight increase in tensile strength (from 30 ± 6 MPa to 38 ± 2 MPa) and elongation at break (from 7 ± 2% to 9 ± 1%) occurred. The toughening may be related to greater nucleation density, resulting in a more homogeneous crystalline morphology, as highlighted in Figure 5. BN addition had no relevant effect on mechanical properties of PHBV18 films, with tensile strength and elongation at break values comprised of the range of 18−20 MPa and 10−13%, respectively. However, the BN addition to PHBV28 led to more contrasted results depending on the amount of added BN. In fact, a reduction of tensile strength and elongation at break values was observed for PHBV28_0.5BN and PHBV28_2BN. However, the addition of 1 wt % BN induced higher tensile strength, stress at break, and similar elongation at break values (120 ± 23% and 122 ± 30% for PHBV28 and PHBV28_1BN, respectively). This observation agreed with DSC and TGA results and corroborated that PHBV28_1BN might be the optimal formulation to ensure the best thermal and mechanical performances. The addition of lower or higher BN amount (0.5 or 2 wt %) to PHBV28 led to worst polymer elongation at break. This could be due to a series of factors including polymer matrix viscosity and specific parameters of the filler such as percolation threshold (ϕ_c). In the case of 0.5 wt % BN addition, the amount of filler is not enough to reach a good mixing in the PHBV28 matrix with respect to PHBV18 and PHBV3 due to hypothetical differences in viscosity and melt flow behavior. On the other hand, the addition of 2 wt % of BN to PHBV28 could lead to a better filler distribution, but probably this value is close to the percolation threshold and the formation of a network between BN particles starts. Agglomerates could be disrupted and filler redispersed by shear forces during mixing processes, but maybe the screw speed used for this work is not enough to ensure filler redispersion.

Effect of mcl-PHA Addition. One of the drawbacks of P3HB and P(3HB-*co*-3HV)s with low 3HV content is the high crystallinity, which limits first mechanical performance but also miscibility with other polymers, particularly amorphous ones. In fact, different crystallinity levels and crystallization kinetics cause phase separation and therefore poor mechanical properties. Modulating P(3HB-*co*-3HV) crystallinity by varying the monomeric composition is a potential solution to immiscibility. Blends of P(3HB-*co*-3HV)s and *mcl*-PHA were

https://doi.org/10.1021/acsomega.4c01282
ACS Omega 2024, 9, 29360−29371

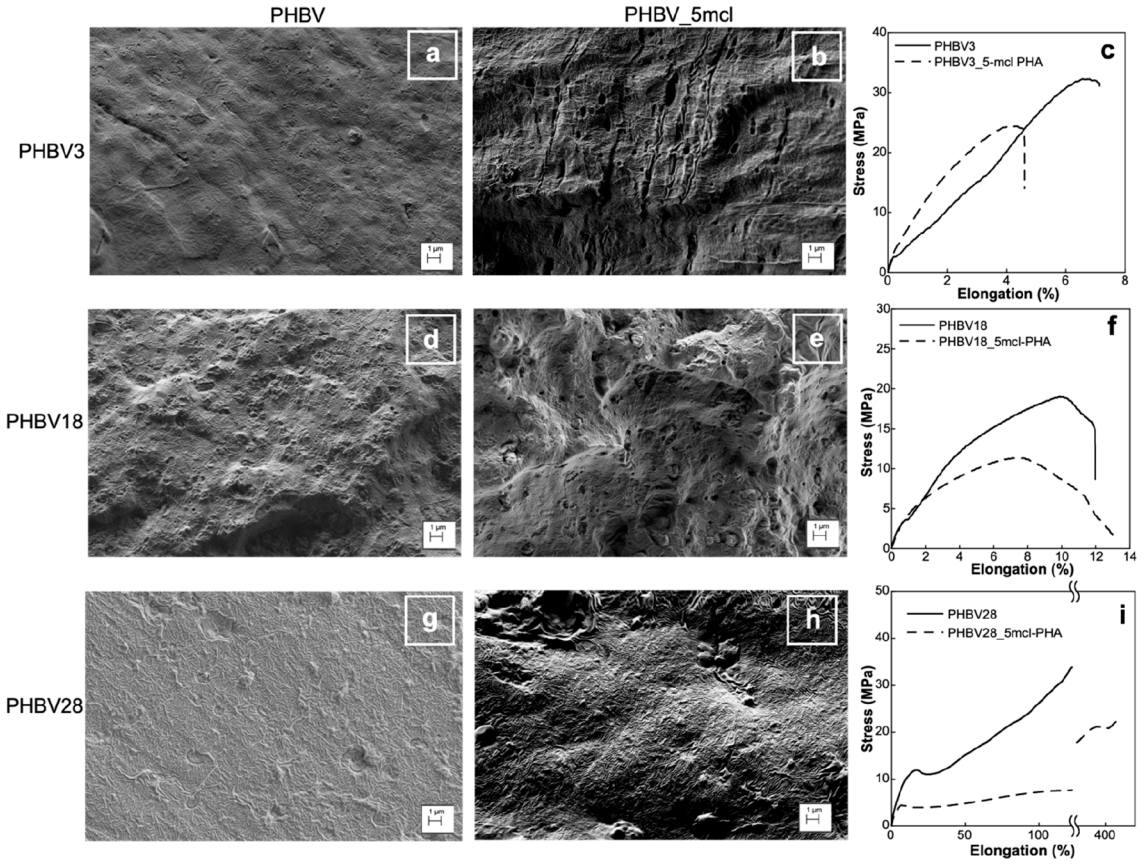

Figure 8. SEM micrographs (10k ×) and stress−strain curves of PHBV3 (a−c), PHBV18 (d−f), and PHBV28 (g−i) materials and respective blends with 5 wt % of mcl-PHA.

prepared and characterized, aiming at the investigation of the effect of monomeric composition on miscibility with other polymers and the obtainment of more flexible films suitable for food packaging applications.

Thermal properties are in general unchanged with respect to the neat PHBV (Figure S9 and Table S1, Supporting Information), but DSC analysis highlighted a plasticizing effect of *mcl*-PHA on PHBV18. In fact, PHBV18_5mcl showed a drop in cold crystallization temperature and melting point, which may be associated with enhanced chain mobility causing a lowering of the activation energy required for cold crystallization. DSC measurements are usually carried out to verify miscibility in binary blends through the presence of a single glass transition (as well as crystallization and melting).[43−45]

Interestingly, there were no multiple thermal transitions in all of the PHBV_5mcl blends. To clarify if this might be ascribed to miscibility or not, TGA analysis has been conducted and data were analyzed using the additive rule according to the equation reported in the Thermal Characterization section. The additive rule consists of a simulation of TGA curve starting from the weighted contribution of each component of a blend[31,46] considering the hypothesis of the interaction and miscibility absence, between components.

Comparison between the simulated and experimental TGA curves is illustrated in Figure 7.

In all cases, the experimental curves of both the single components and blends exhibited only one weight loss. Regarding thermal stability, it is worth noting that *mcl*-PHA thermodegradation starts at a lower temperature than PHBV3 (261 °C for *mcl*-PHA with respect to 270 °C for PHBV3), while it was more thermally stable than PHBV18 (223 °C) and PHBV28 (234 °C). Mixing PHBV3 and *mcl*-PHA does not result in noticeable changes in thermal stability. No difference between experimental and simulated curves was observed for PHBV3_5mcl, meaning that according to the additive rule, PHBV3 and *mcl*-PHA were not miscible. The reason for this behavior could be the independent crystallization of the two phases after cooling, which results in macrophase separation. In contrast, PHBV18_5mcl and PHBV28_5mcl experimental curves showed that degradation started at 254 and 264 °C, respectively. Thus the addition of 5 wt % *mcl*-PHA to PHBV18 or PHBV28 led to the formation of blends with higher thermal stability than P(3HB-*co*-3HV)s alone (degradation starts at 223 and 234 °C for PHBV18 and PHBV28, respectively). Comparing the experimental and simulated curves, it emerges that the blends are more thermally stable because degradation started at higher temperatures than predicted (229 and 238 °C for PHBV18_5mcl and PHBV28_5mcl, respectively). The discrepancy between the experimental and simulated results suggests that *mcl*-PHA may interact with P(3HB-*co*-3HV) with higher 3HV concentrations. The crystallization rate is lower for P(3HB-*co*-3HV) copolymers with higher contents of 3HV units, which favors miscibility with a more amorphous polymer, as is the case for PHBV18_5mcl and mainly for PHBV28_5mcl. This has the advantage of avoiding a quick exclusion of the noncrystalline component from melted blend.

Regarding Figure 8, it appears that the immiscibility implies a worsening in morphology and mechanical properties, i.e.,

https://doi.org/10.1021/acsomega.4c01282
ACS Omega 2024, 9, 29360−29371

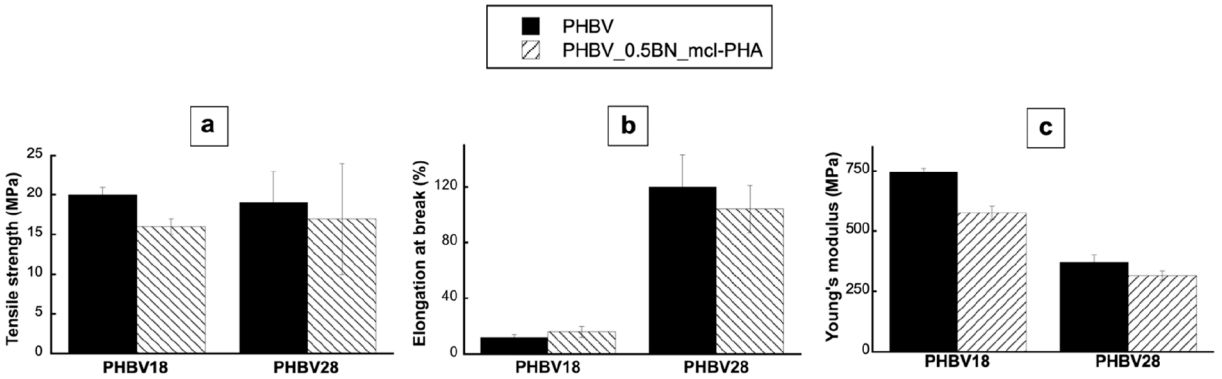

Figure 9. Mechanical properties of PHBV_0.5BN_5mcl ternary compounds: (a) Tensile strength (MPa), (b) elongation at break (%), and (c) Young's modulus (MPa).

Young's modulus and tensile strength, of all P(3HB-*co*-3HV)/*mcl*-PHA blends.

Morphological analysis by scanning electron microscopy confirmed the hypothesis that P(3HB-*co*-3HV)s are characterized by different compatibility with *mcl*-PHA depending on their monomeric composition. PHBV3 (Figures 8a and 8b) exhibited a droplet-matrix-like morphology typical of immiscible blends. The holes are caused by the segregation of the amorphous polymer, which leads to the formation of two macrophases and thus to the formation of interfaces that may serve as preferred planes for fracture, causing the reduction of elongation at break values (Figure 8c). The SEM results show that PHBV18_5mcl exhibits an irregular morphology (Figures 8d and 8e) and a drop in tensile strength of almost 50% (Figure 8f), reminiscent of an immiscible binary blend. However, increasing the 3HV content to 28 mol % resulted in a more regular morphology and different mechanical properties than in the case of PHBV28_5mcl, which showed no droplet-matrix-like structure (Figures 8g and 8h) and an improvement in elongation at break, which increased from 120 ± 23% to 400 ± 200% (Figure 8i).

It is worth noting that the images reported in Figure S8 of Supporting Information show that PHBV18_5mcl and PHBV28_5mcl films are transparent. Transparency is a key factor in the selection of food packaging materials that allow the consumer to see the product inside and check its physical condition.

Therefore, mechanical and morphological results are in good agreement with the thermal characterization results, which show different degrees of compatibility of P(3HB-*co*-3HV)/*mcl*-PHA depending on the 3HV unit content. PHBV28 is compatible with a more amorphous copolymer (*mcl*-PHA) and combining these two PHAs enables the creation of a material with improved flexibility and qualities suited for food packaging, according to all of the data.

Synergistic Effect of BN and mcl-PHA Addition. The results illustrated in previous sections highlighted the effectiveness of BN addition in reducing melt crystallization time and enhancing processability, while *mcl*-PHA thanks to its compatibility with higher 3HV content P(3HB-*co*-3HV) contributed to improve elongation at break and transparency. Considering all the above, synergistic reinforcement of PHBV18 and PHBV28 by adding both the BN and *mcl*-PHA was assessed by preparing ternary compounds of P(3HB-*co*-3HV) with 0.5 wt % BN and 5 wt % *mcl*-PHA. Despite that the addition of 1 wt % of BN leads to the best results, a minimum BN quantity (0.5 wt %) has been used to verify if the simultaneous presence of *mcl*-PHA could result in a different dispersion due to a change in polymer matrix viscosity.

PHBV3 has not been tested because its excessive crystallinity did not allow production of a miscible blend; the simultaneous addition of both BN and *mcl*-PHA could result in higher immiscibility and worse properties.

The positive effects of BN and *mcl*-PHA on thermal stability illustrated in the previous section were also maintained when added simultaneously, as the increasing of T_d^{onset} with respect to neat polymers demonstrates (PHBV18 passes from 223 ± 1 to 250 ± 5 °C, while PHBV28 passes from 234 ± 3 to 262 °C) (Table S1 and Figure S11, Supporting Information). On the other hand, no effect on thermal properties analyzed by DSC (Table S1 and Figure S10, Supporting Information) was detected. For example, PHBV18 melting temperature is 125 ± 2 °C (1st peak) and 164 ± 1 °C (2nd peak) and it is comparable to PHBV18_0.5BN_5mcl (124 ± 1 °C first peak, 163 ± 1 °C second peak).

The production of a ternary compound had nearly no impact on the mechanical properties (Figure 9) with just a few changes in PHBV18 properties.

The Young's modulus and tensile strength of PHBV28 decreased from 746 ± 15 MPa to 575 ± 27 MPa and from 20 ± 1 to 15 ± 1 MPa, respectively, while the elongation at break remained fairly constant (12 ± 2% to 16 ± 4% for neat PHBV18 and ternary PHBV18 compounds, respectively). The mechanical properties of PHBV28 remained high, indicating that the addition of a nucleating agent and an amorphous polymer did not deteriorate the native properties, which have the advantage of greater thermal stability. The mechanical properties are affected by high standard deviation values, indicating some heterogeneity within the materials. This was ascribed to the poor distribution of *mcl*-PHA and BN when added simultaneously to the P(3HB-*co*-3HV) matrix.

WVP Measurements. Water vapor permeability (WVP) measurements were carried out on both neat and formulated P(3HB-*co*-3HV)-based films (Table 4) to assess whether the monomeric composition as well as the formulation can affect one of the main barrier properties of primary packaging, that is, the water vapor barrier. The WVP of the neat PHBV3 film, $7.3.10^{-13}$ mol m^{-1} s^{-1} $Pa^{-}1$, was close to previous results reported in literature.[47] Despite the correlation between 3HV content and crystallinity, which in turn affected other properties as discussed in the Effect of 3HV Content on Processability and Mechanical Properties section, it is worth

https://doi.org/10.1021/acsomega.4c01282
ACS Omega 2024, 9, 29360−29371

Table 4. WVP Values of P(3HB-*co*-3HV)-Based Films

sample	WVP (mol m^{-1} s^{-1} Pa^{-1})		
PHBV3	7.3×10^{-13}	±	1.9×10^{-13}
PHBV3_0.5BN	5.1×10^{-13}	±	9.4×10^{-14}
PHBV3_5mcl	4.4×10^{-13}	±	1.2×10^{-13}
PHBV18	6.8×10^{-13}	±	1.5×10^{-13}
PHBV18_0.5BN	7.1×10^{-13}	±	1.5×10^{-13}
PHBV18_1BN	5.3×10^{-13}	±	9.6×10^{-14}
PHBV18_5mcl	6.8×10^{-13}	±	8.5×10^{-14}
PHBV18_0.5BN_5mcl	6.5×10^{-13}	±	1.1×10^{-13}
PHBV28	6.5×10^{-13}	±	1.1×10^{-13}
PHBV28_0.5BN	6.7×10^{-13}	±	7.1×10^{-14}
PHBV28_1BN	6.7×10^{-13}	±	1.0×10^{-13}
PHBV28_2BN	8.7×10^{-13}	±	1.2×10^{-13}
PHBV28_5mcl	6.4×10^{-13}	±	1.5×10^{-13}
PHBV28_0.5BN_5mcl	6.6×10^{-13}	±	1.3×10^{-13}

noting that WVP was not significantly impacted by the different monomeric compositions or by the addition of BN or *mcl*-PHA (or both). This agrees with the study by Miguel and Iruin[47] on the characterization of water sorption and transport in P3HB and its copolymers with various 3HV contents. The constancy of WVP demonstrates that it is possible to improve the thermal and mechanical properties of P(3HB-*co*-3HV) without significantly affecting the original barrier properties. This shows that the observed changes in the microstructure (in the range of tested 3HV contents) do not significantly affect either diffusion or sorption phenomena.

CONCLUSIONS

In the present work, the influence of 3-hydroxyvalerate (3HV) content (3, 18 and 28%mol) on the processability and final properties of P(3HB-*co*-3HV)-based films was investigated. In terms of ductility improvement, it was shown that a 3HV content of 28 mol % was optimal. The entanglement of the polymer chains by a compounding step (melt extrusion) was demonstrated to be necessary to further improve the ductility of P(3HB-*co*-3HV) with a higher 3HV unit concentration. The films produced from PHBV28 showed a 3-fold higher elongation at break of 120% compared to nonextruded films.

However, since the increase in the 3HV unit content causes a decrease in the crystallization rate, the nucleating effect of boron nitride (BN) added in different quantities has been investigated. It was found that the optimal amount of BN depended on the monomeric composition. A threshold limit of 1 wt % BN has been individuated for PHBV28 above which BN particles seemed to aggregate. Optimal mechanical properties were determined, particularly values of tensile strength of 13 ± 1 MPa, Young's modulus of 393 ± 13%, and elongation at break of 122 ± 16%. Despite the slightly higher nucleation efficiency ($\Delta T_{mc} = 9$ °C), the addition of BN was insufficient to significantly improve the mechanical properties of virgin P(3HB-*co*-3HV). However, it appeared as a way to strengthen the thermal stability (T_d^{onset} increased from 234 ± 3 to 263 ± 0.7 °C).

The elongation at break of PHBV28 blended with 5% *mcl*-PHA reached 400 ± 200%, demonstrating the potential flexibility of P(3Hb-*co*-3HV) when mixed with more amorphous biopolymers that serve as plasticizers. The good compatibility between PHBV28 and *mcl*-PHA could be attributed to the slow crystallization of P(3HB-*co*-3HV), which prevents phase separation. However, the preparation of a ternary P(3HB-*co*-3HV) compound with 0.5% BN and 5% *mcl*-PHA did not lead to noticeably improved properties, except for the thermal stability. Ductility was not improved compared to the virgin polymer or PHBV28_1BN. Finally, it should be noted that the barrier properties of all formulations tested were not affected by either the 3HV content or additives.

This work provides clarity on copolymers with different 3HV contents and proposes interesting solutions to overcome the drawbacks related to low processability and ductility and to obtain a potential biobased and biodegradable material for packaging applications. This could be particularly interesting in view of the use of PHBV for extrusion coatings.

ASSOCIATED CONTENT

Data Availability Statement

Some research data will be made available in the following repository upon acceptance of the article: https://entrepot.recherche.data.gouv.fr/dataverse/loop4pack.

Supporting Information

The Supporting Information is available free of charge at https://pubs.acs.org/doi/10.1021/acsomega.4c01282.

Thermal properties values (Table S1), DSC thermograms, TGA traces and pictures of all formulations (Figures S1−S11) (PDF)

AUTHOR INFORMATION

Corresponding Author

Hélène Angellier-Coussy − *JRU IATE 1208, INRAE, Montpellier SupAgro, University of Montpellier, 34060 Montpellier, France*; Email: helene.coussy@umontpellier.fr

Authors

Sara Alfano − *Department of Chemistry, University of Rome La Sapienza, 00185 Rome, Italy*; orcid.org/0000-0002-8460-800X

Estelle Doineau − *JRU IATE 1208, INRAE, Montpellier SupAgro, University of Montpellier, 34060 Montpellier, France*

Coline Perdrier − *JRU IATE 1208, INRAE, Montpellier SupAgro, University of Montpellier, 34060 Montpellier, France*

Laurence Preziosi-Belloy − *JRU IATE 1208, INRAE, Montpellier SupAgro, University of Montpellier, 34060 Montpellier, France*

Nathalie Gontard − *JRU IATE 1208, INRAE, Montpellier SupAgro, University of Montpellier, 34060 Montpellier, France*

Andrea Martinelli − *Department of Chemistry, University of Rome La Sapienza, 00185 Rome, Italy*; orcid.org/0000-0002-6401-9988

Estelle Grousseau − *JRU IATE 1208, INRAE, Montpellier SupAgro, University of Montpellier, 34060 Montpellier, France*

Complete contact information is available at: https://pubs.acs.org/10.1021/acsomega.4c01282

Funding

This work was performed in the framework of the LOOP4-PACK project https://projet-loop4pack.fr/en/welcome/ which is supported by the French National Research Agency (ANR) [Grant Agreement N#ANR-19-CE43-0006].

Notes

The authors declare no competing financial interest.

■ ACKNOWLEDGMENTS

The LOOP4PACK project [Grant Agreement N#ANR-19-CE43-0006] is kindly acknowledged for the funding support. The authors would thank Dr. Gianluca Zanellato and CNIS—Centro di Ricerca per le nanotecnologie for SEM images.

■ REFERENCES

(1) Arcos-Hernandez, M. v.; Laycock, B.; Pratt, S.; Donose, B. C.; Nikolič, M. A. L.; Luckman, P.; Werker, A.; Lant, P. A. Biodegradation in a Soil Environment of Activated Sludge Derived Polyhydroxyalkanoate (PHBV). *Polym. Degrad. Stab.* **2012**, *97* (11), 2301−2312.

(2) Valentino, F.; Gottardo, M.; Micolucci, F.; Pavan, P.; Bolzonella, D.; Rossetti, S.; Majone, M. Organic Fraction of Municipal Solid Waste Recovery by Conversion into Added-Value Polyhydroxyalkanoates and Biogas. *ACS Sustainable Chem. Eng.* **2018**, *6*, 16375.

(3) Lorini, L.; Munarin, G.; Salvatori, G.; Alfano, S.; Pavan, P.; Majone, M.; Valentino, F. Sewage Sludge as Carbon Source for Polyhydroxyalkanoates: A Holistic Approach at Pilot Scale Level. *J. Clean Prod.* **2022**, *354*, 131728.

(4) Elain, A.; le Grand, A.; Corre, Y. M.; le Fellic, M.; Hachet, N.; le Tilly, V.; Loulergue, P.; Audic, J. L.; Bruzaud, S. Valorisation of Local Agro-Industrial Processing Waters as Growth Media for Polyhydroxyalkanoates (PHA) Production. *Ind. Crops Prod* **2016**, *80*, 1−5.

(5) Montemurro, M.; Salvatori, G.; Alfano, S.; Martinelli, A.; Verni, M.; Pontonio, E.; Villano, M.; Rizzello, C. G. Exploitation of Wasted Bread as Substrate for Polyhydroxyalkanoates Production through the Use of Haloferax Mediterranei and Seawater. *Front. Microbiol.* **2022**, DOI: 10.3389/fmicb.2022.1000962.

(6) Laycock, B.; Halley, P.; Pratt, S.; Werker, A.; Lant, P. The Chemomechanical Properties of Microbial Polyhydroxyalkanoates. *Prog. Polym. Sci.* **2013**, *38*, 536−583.

(7) Park, S. J.; Kim, T. W.; Kim, M. K.; Lee, S. Y.; Lim, S. C. Advanced Bacterial Polyhydroxyalkanoates: Towards a Versatile and Sustainable Platform for Unnatural Tailor-Made Polyesters. *Biotechnol Adv.* **2012**, *30* (6), 1196−1206.

(8) Owen, A. J.; Heinzel, J.; Škrbić, Ž.; Divjaković, V. Crystallization and Melting Behaviour of PHB and PH B/HV Copolymer. *Polymers* **1992**, *33* (7), 1563−1567.

(9) Ariffin, H.; Nishida, H.; Shirai, Y.; Hassan, M. A. Determination of Multiple Thermal Degradation Mechanisms of Poly(3-Hydroxybutyrate). *Polym. Degrad. Stab.* **2008**, *93* (8), 1433−1439.

(10) Hobbs, J. K.; Barham, P. J. The Fracture of Poly-(Hydroxybutyrate) Part III Fracture Morphology in Thin Films and Bulk Systems. *J. Mater. Sci.* **1999**, *34* (19), 4831−4844.

(11) Sängerlaub, S.; Brüggemann, M.; Rodler, N.; Jost, V.; Bauer, K. D. Extrusion Coating of Paper with Poly(3-Hydroxybutyrate-Co-3-Hydroxyvalerate) (PHBV)—Packaging Related Functional Properties. *Coatings* **2019**, *9* (7), 457.

(12) Srubar, W. V.; Wright, Z. C.; Tsui, A.; Michel, A. T.; Billington, S. L.; Frank, C. W. Characterizing the Effects of Ambient Aging on the Mechanical and Physical Properties of Two Commercially Available Bacterial Thermoplastics. *Polym. Degrad. Stab.* **2012**, *97* (10), 1922−1929.

(13) Ferre-Guell, A.; Winterburn, J. Biosynthesis and Characterization of Polyhydroxyalkanoates with Controlled Composition and Microstructure. *Biomacromolecules* **2018**, *19* (3), 996−1005.

(14) Perdrier, C.; Doineau, E.; Leroyer, L.; Subileau, M.; Angellier-Coussy, H.; Preziosi-Belloy, L.; Grousseau, E. Impact of Overflow vs. Limitation of Propionic Acid on Poly(3-Hydroxybutyrate-Co-3-Hydroxyvalerate) Biosynthesis. *Process Biochemistry* **2023**, *128*, 147−157.

(15) Wang, Y.; Yamada, S.; Asakawa, N.; Yamane, T.; Yoshie, N.; Inoue, Y. Comonomer Compositional Distribution and Thermal and Morphological Characteristics of Bacterial Poly(3-Hydroxybutyrate-Co-3-Hydroxyvalerate)s with High 3-Hydroxyvalerate Content. *Biomacromolecules* **2001**, *2* (4), 1315−1323.

(16) Ye, H. M.; Xu, J.; Guo, B. H.; Iwata, T. Left- or Right-Handed Lamellar Twists in Poly[(R)-3-Hydroxyvalerate] Banded Spherulite: Dependence on Growth Axis. *Macromolecules* **2009**, *42* (3), 694−701.

(17) Melendez-Rodriguez, B.; Reis, M. A. M.; Carvalheira, M.; Sammon, C.; Cabedo, L.; Torres-Giner, S.; Lagaron, J. M. Development and Characterization of Electrospun Biopapers of Poly(3-Hydroxybutyrate- Co-3-Hydroxyvalerate) Derived from Cheese Whey with Varying 3-Hydroxyvalerate Contents. *Biomacromolecules* **2021**, *22* (7), 2935−2953.

(18) Abbasi, M.; Pokhrel, D.; Coats, E. R.; Guho, N. M.; McDonald, A. G. Effect of 3-Hydroxyvalerate Content on Thermal, Mechanical, and Rheological Properties of Poly(3-Hydroxybutyrate-Co-3-Hydroxyvalerate) Biopolymers Produced from Fermented Dairy Manure. *Polymers (Basel)* **2022**, *14* (19), 4140.

(19) Doineau, E.; Perdrier, C.; Allayaud, F.; Blanchet, E.; Preziosi-Belloy, L.; Grousseau, E.; Gontard, N.; Angellier-Coussy, H. Designing Poly(3-Hydroxybutyrate-Co-3-Hydroxyvalerate) P(3HB-Co-3HV) Films with Tailored Mechanical Properties. *Mater. Today Commun.* **2023**, *36*, 106848.

(20) Langford, A.; Chan, C. M.; Pratt, S.; Garvey, C. J.; Laycock, B. The Morphology of Crystallisation of PHBV/PHBV Copolymer Blends. *Eur. Polym. J.* **2019**, *112*, 104−119.

(21) Miao, Y.; Fang, C.; Shi, D.; Li, Y.; Wang, Z. Coupling Effects of Boron Nitride and Heat Treatment on Crystallization, Mechanical Properties of Poly (3-Hydroxybutyrate-Co-3-Hydroxyvalerate) (PHBV). *Polymer* **2022**, *252*, 124967.

(22) Carli, L. N.; Crespo, J. S.; Mauler, R. S. PHBV Nanocomposites Based on Organomodified Montmorillonite and Halloysite: The Effect of Clay Type on the Morphology and Thermal and Mechanical Properties. *Compos Part A Appl. Sci. Manuf* **2011**, *42* (11), 1601−1608.

(23) Seoane, I. T.; Fortunati, E.; Puglia, D.; Cyras, V. P.; Manfredi, L. B. Development and Characterization of Bionanocomposites Based on Poly(3-Hydroxybutyrate) and Cellulose Nanocrystals for Packaging Applications. *Polym. Int.* **2016**, *65* (9), 1046−1053.

(24) Kai, W.; He, Y.; Inoue, Y. Fast Crystallization of Poly(3-hydroxybutyrate) and Poly(3-hydroxybutyrate-co-3-hydroxyvalerate) with Talc and Boron Nitride as Nucleating Agents. *Polym. Int.* **2005**, *54* (5), 780−789.

(25) Don, T.-M.; Chung, C.-Y.; Lai, S.-M.; Chiu, H.-J. Preparation and Properties of Blends from Poly(3-Hydroxybutyrate) with Poly(Vinyl Acetate)-Modified Starch. *Polym. Eng. Sci.* **2010**, *50* (4), 709−718.

(26) Modi, S. J.; Cornish, K.; Koelling, K.; Vodovotz, Y. Fabrication and Improved Performance of Poly(3-Hydroxybutyrate-Co-3-Hydroxyvalerate) for Packaging by Addition of High Molecular Weight Natural Rubber. *J. Appl. Polym. Sci.* **2016**, DOI: 10.1002/app.43937.

(27) Zhao, X.; Venoor, V.; Koelling, K.; Cornish, K.; Vodovotz, Y. Bio-based Blends from Poly(3-hydroxybutyrate-*co*-3-hydroxyvalerate) and Natural Rubber for Packaging Applications. *J. Appl. Polym. Sci.* **2019**, DOI: 10.1002/app.47334.

(28) Ha, C. S.; Cho, W. J. Miscibility, Properties, and Biodegradability of Microbial Polyester Containing Blends. *Prog. Polym. Sci.* **2002**, *27* (4), 759−809.

(29) Yu, L.; Dean, K.; Li, L. Polymer Blends and Composites from Renewable Resources. *Prog. Polym. Sci.* **2006**, *31* (6), 576−602.

(30) Feijoo, P.; Samaniego-Aguilar, K.; Sánchez-Safont, E.; Torres-Giner, S.; Lagaron, J. M.; Gamez-Perez, J.; Cabedo, L. Development and Characterization of Fully Renewable and Biodegradable Polyhydroxyalkanoate Blends with Improved Thermoformability. *Polymers (Basel)* **2022**, *14* (13), 2527.

(31) Martelli, S. M.; Sabirova, J.; Fakhouri, F. M.; Dyzma, A.; de Meyer, B.; Soetaert, W. Obtention and Characterization of Poly(3-Hydroxybutyricacid-Co-Hydroxyvaleric Acid)/Mcl-PHA Based Blends. *LWT* **2012**, *47* (2), 386−392.

https://doi.org/10.1021/acsomega.4c01282
ACS Omega 2024, 9, 29360−29371

(32) Sadi, R. K.; Kurusu, R. S.; Fechine, G. J. M.; Demarquette, N. R. Compatibilization of Polypropylene/Poly(3-Hydroxybutyrate) Blends. *J. Appl. Polym. Sci.* **2012**, *123* (6), 3511−3519.
(33) Przybysz, M.; Marć, M.; Klein, M.; Saeb, M. R.; Formela, K. Structural, Mechanical and Thermal Behavior Assessments of PCL/PHB Blends Reactively Compatibilized with Organic Peroxides. *Polym. Test* **2018**, *67*, 513−521.
(34) Perdrier, C.; Doineau, E.; Leroyer, L.; Subileau, M.; Angellier-Coussy, H.; Preziosi-Belloy, L.; Grousseau, E. Impact of Overflow vs. Limitation of Propionic Acid on Poly(3-Hydroxybutyrate-Co-3-Hydroxyvalerate) Biosynthesis. *Process Biochemistry* **2023**, *128*, 147.
(35) Bossu, J.; Le Moigne, N.; Dieudonné-George, P.; Dumazert, L.; Guillard, V.; Angellier-Coussy, H. Impact of the Processing Temperature on the Crystallization Behavior and Mechanical Properties of Poly[R-3-Hydroxybutyrate-Co-(R-3-Hydroxyvalerate)]. *Polymer* **2021**, *229*, 123987.
(36) Mitomo, H.; Barham, P. J.; Keller, A. Crystallization and Morphology of Poly(p-Hydroxybutyrate) and Its Copolymer. *Polym. J.* **1987**, *19*, 1241.
(37) Anderson, K. S.; Hillmyer, M. A. Melt Preparation and Nucleation Efficiency of Polylactide Stereocomplex Crystallites. *Polymer (Guildf)* **2006**, *47* (6), 2030−2035.
(38) Song, P.; Wei, Z.; Liang, J.; Chen, G.; Zhang, W. Crystallization Behavior and Nucleation Analysis of Poly(L-lactic Acid) with a Multiamide Nucleating Agent. *Polym. Eng. Sci.* **2012**, *52* (5), 1058−1068.
(39) Liu, W. J.; Yang, H. L.; Wang, Z.; Dong, L. S.; Liu, J. J. Effect of Nucleating Agents on the Crystallization of Poly(3-Hydroxybutyrate-Co-3-Hydroxyvalerate). *J. Appl. Polym. Sci.* **2002**, *86* (9), 2145−2152.
(40) Kai, W.; He, Y.; Inoue, Y. Fast Crystallization of Poly(3-Hydroxybutyrate) and Poly(3-Hydroxybutyrate-Co-3-Hydroxy-Valerate) with Talc and Boron Nitride as Nucleating Agents. *Polymer International Polym. Int.* **2005**, *54*, 780−789.
(41) Chen, G. X.; Hao, G. J.; Guo, T. Y.; Song, M. D.; Zhang, B. H. Structure and Mechanical Properties of Poly(3-Hydroxybutyrate-Co-3-Hydroxyvalerate) (PHBV)/Clay Nanocomposites. *J. Mater. Sci. Lett.* **2002**, *21* (20), 1587−1589.
(42) Yu, J.; Huang, X.; Wu, C.; Wu, X.; Wang, G.; Jiang, P. Interfacial Modification of Boron Nitride Nanoplatelets for Epoxy Composites with Improved Thermal Properties. *Polymer (Guildf)* **2012**, *53* (2), 471−480.
(43) Focarete, M. L.; Ceccorulli, G.; Scandola, M.; Kowalczuk, M. Further Evidence of Crystallinity-Induced Biodegradation of Synthetic Atactic Poly(3-Hydroxybutyrate) by PHB-Depolymerase A from Pseudomonas Lemoignei. Blends of Atactic Poly(3-Hydroxybutyrate) with Crystalline Polyesters. *Macromolecules* **1998**, *31* (24), 8485−8492.
(44) Jenkins, M. J.; Cao, Y.; Howell, L.; Leeke, G. A. Miscibility in Blends of Poly(3-Hydroxybutyrate-Co-3-Hydroxyvalerate) and Poly-(ε-Caprolactone) Induced by Melt Blending in the Presence of Supercritical CO2. *Polymer (Guildf)* **2007**, *48* (21), 6304−6310.
(45) Wang, X.; Chen, Z.; Chen, X.; Pan, J.; Xu, K. Miscibility, Crystallization Kinetics, and Mechanical Properties of Poly(3-Hydroxybutyrate-Co-3-Hydroxyvalerate)(PHBV)/Poly(3-Hydroxybutyrate-Co-4- Hydroxybutyrate)(P3/4HB) Blends. *J. Appl. Polym. Sci.* **2010**, *117* (2), 838−848.
(46) Dodson, B.; McNeill, I. C. Degradation of Polymer Mixtures. VI. Blends of Poly(Vinyl Chloride) with Polystyrene. *Journal of Polymer Science: Polymer Chemistry Edition* **1976**, *14* (2), 353−364.
(47) Miguel, O.; Iruin, J. J. Water Transport Properties in Poly(3-Hydroxybutyrate) and Poly(3-Hydroxybutyrate-Co-3-Hydroxyvalerate) Biopolymers. *J. Appl. Polym. Sci.* **1999**, *73* (4), 455−468.

https://doi.org/10.1021/acsomega.4c01282
ACS Omega 2024, 9, 29360−29371